VOL. 20, NO. 2-3, 2021, 103-106
www.elektrika.utm.my
ISSN 0128-4428

ELEKTRIKA
Journal of Electrical Engineering

MCNPX Modelling and Simulation of Point-source Detection using Different iSPECT Geometrical Arrangement

Hanafi Ithnin[1,2], **Elmy Johanna Mohamad** [1*], **Norliana Mohd Lip** [3] and **Nazrul Hizam Yusoff** [2]

[1]Faculty of Electrical Engineering, Universiti Tun Hussein Onn, 86400 Batu Pahat, Johor, Malaysia.
[2]Industrial Technology Division, Malaysian Nuclear Agency, 43000, Kajang, Selangor, Malaysia.
[3]Faculty of Computer and Mathematical Science, Universiti Teknologi MARA, 70300 Negeri Sembilan, Malaysia.

[*]Corresponding author: elmy@uthm.edu.my, Tel: 607-453 3453

Abstract: Single photon emission computed tomography, SPECT, has been proven reliable in imaging radiotracer distribution inside an opaque system. Due to the limited number of detection tools available, an assessment and comparison are made for different detection arrangement in developing an industrial SPECT system (iSPECT) which can be utilized for imaging in industrial condition. In the present study, hexagonal, octagonal and nonagonal iSPECT arrangements were modelled and simulated using MCNPX code. The detection system only used a maximum number of 36 lead collimated sodium iodide, NaI scintillation detector. The reconstructed images for single point-source and two point-source are evaluated and compared for all three systems. The result shows of the three iSPECT arrangement, the nonagonal system has the best image resolution and ability to detect the single and two point-source position inside the region of interest.

Keywords: Emission tomography, Industrial SPECT, Point-source imaging.

Article History: received 25 May 2021; accepted 12 June 2021; published 15 October 2021.

1. INTRODUCTION

Single photon emission tomography system, SPECT, has been used extensively in the medical application as a tool for diagnosing functionality of the human internal organ. Thus, the development of the medical SPECT system has been very advance. Recently the demand for using SPECT in the industry has been growing due to the fact that SPECT system can image the distribution of radiotracer in an opaque system. This imaging system will benefit the industry in visualizing the flow regime, flow distribution and dead zone in a flow process. However, the lack of application of SPECT in industrial is due to the dependence on the environmental condition of industrial problems where the different interest of problems needs different setup for the SPECT system. Thus, this study is aimed to simulate an industrial SPECT system, iSPECT, for imaging laminar flow in a pipeline using MCNPX code.

Several studies were made to demonstrate the possibility of using the SPECT system to be used in industrial problems. Legoupil et al. [1] did the earliest of such work, where an experimental SPECT system was developed for dynamic fluid flow analysis. The results were promising where the 2D image of the radiotracer distribution successfully constructed. Several works in the development of different types of industrial SPECT system by experimental and modelling and simulations [2-4]. More recent works were done by Park et al. [5], where they made an industrial SPECT system with a 12-gonal diverging collimator and compared it with 24-gonal and hexagonal SPECT system. The results show that the 12-gonal system offered the best performance, providing a detection-efficiency map without edge artefacts, the best image resolution, and reconstruction images that correctly furnish multi-source information. This shows that different interest of problems requires different setup of industrial SPECT system, where several different numbers of detectors and different arrangement of the detector arrays should be considered.

The works in the present study involve modelling and simulation of three arrangement of industrial SPECT system, iSPECT, which are hexagonal, octagonal and nonagonal system. For the purpose of developing the iSPECT hardware in future, this simulation study is limited to use only a maximum number of 36 Sodium Iodide, NaI scintillation detectors. The simulation will assess the single point-source positional mapping accuracy on the reconstructed image inside a 20 cm region of interest. Cesium, Cs-137 gamma-ray source with the energy of 622 keV is used in this study to simulate the point-source. This study also presents the reconstructed images of two point-source mappings simultaneously and compares the reconstructed images of the three iSPECT system

arrangement.

2. METHODOLOGY

2.1 Modelling the iSPECT system

In this study, the iSPECT system is modelled and simulated using the Monte Carlo N-Particle eXtended, MCNPX code [6]. The MCNPX code is a general-purpose Monte Carlo radiation transport code with three-dimensional geometry and continuous- energy transport of particles and light ions. The code is used for modelling the iSPECT detectors and detection process of the gamma-ray from radiotracer. In this study, the number of detectors used is limited to a maximum of 36 NaI scintillation detectors. Thus, the available simulations for the iSPECT system for three different arrangement are hexagonal - six arrays of six detectors (6x6), octagonal - eight arrays of four detectors (8x4), and nonagonal - nine arrays of four detectors (9x4). Figure 1 shows the model of iSPECT made using McPlot from the MCNPX package.

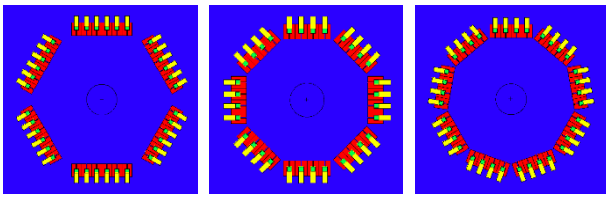

(a) (b) (c)

Figure 1: Three different model of iSPECT system used in this study; (a)hexagonal (6x6), (b) octagonal (8x4) and (c) nonagonal (9x4).

2.2 Detector and Collimators

Each detector used in this study is a 1-inch NaI scintillation detector, with each detector is collimated with a 3.5 cm lead collimator and 0.5 cm collimator hole width. Figure 2 shows the model of a single NaI scintillation detector with its lead collimator.

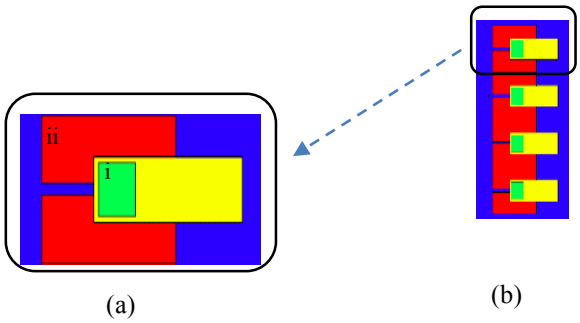

(a) (b)

Figure 2: (a) Single NaI scintillation model with (i) is detector crystal and (ii) is the lead collimator and (b) Four detectors arrange in an array for iSPECT simulation.

In designing the collimator for the iSPECT system, the general rule is to consider the profile obtained with a source moving along the diameter of the region of interest (ROI) that is parallel to the projection. The relevant parameter is the full-width at half maximum, FWHM of the measurement profile of the moving source [7]. A good condition for collimator design given in Equation 1

$$1 \leq \frac{FWHM\ x\ No\ of\ detectors}{Diameter\ ROI} \leq 2 \quad (1)$$

whare,

$$FWHM = \frac{Col.hole\ width\ x\ Dis.detector\ to\ column\ ctr}{Col.hole\ depth} \quad (2)$$

In the present study, the collimator used for all three systems should be in a good range for scanning area in the range present in Table 1. Thus, the simulation of the iSPECT system will consider the scanned region or region of interest with 20 cm diameter, which is in a good condition range for all three arrangements.

Table 1. Condition for a range of ROI from the collimator

iSPECT system	ROI range (cm)
Hexagonal	20 - 41
Octagonal	11 - 23
Nonagonal	12 - 25

2.3 Image Reconstruction and Point-source Simulation

Due to the limited number of detectors in an array, the iterative reconstruction method is selected for producing a high-resolution image in the present study. There are several iterative algorithms for reconstructing the iSPECT image. In this study, the Maximum Likelihood – Expectation Maximization (ML-EM) [8,9] method was used for reconstructing the iSPECT image. The iterative equation of the ML-EM method is denoted in Equation 3.

$$y^{(n+1)} = \frac{y_j^{(n)}}{\sum_{i'} h_{i'j}} \sum_i h_{ij} \frac{g_i}{\sum_k h_{ik} y_k^{(n)}} \quad (3)$$

The unknown image of radiotracer distribution y is determined by the iSPECT detector count g and the system matrix h, which is the probability distribution that photons emitted from the jth pixel registered in the ith detector. The ML-EM algorithm has several advantages over other algorithms, as mention by Park *et al.* [5]. First, the gamma-ray emission and detection are based on Poisson distribution, which is the same for the ML-EM algorithm. Subsequently, the reconstruction process of the ML-EM algorithm gives better diagnostic performance over the conventional filtered back-projection FBP method. Finally, the error and updates are multiplicative; thus, ML-EM automatically imposes a nonnegativity constraint and allows for selected pixels to be preset to zero.

For each of the three arrangements, the pixel interval is set as 0.5 cm for 20 cm diameter of a circular region of interest, ROI. Thus, a total of 1245 points source response needed to be calculated, as shown in Figure 3(a). This point-source response is the input for the system matrix, *h,* in the ML-EM algorithm used for calculating the reconstructed image of radiotracer distribution *y*.

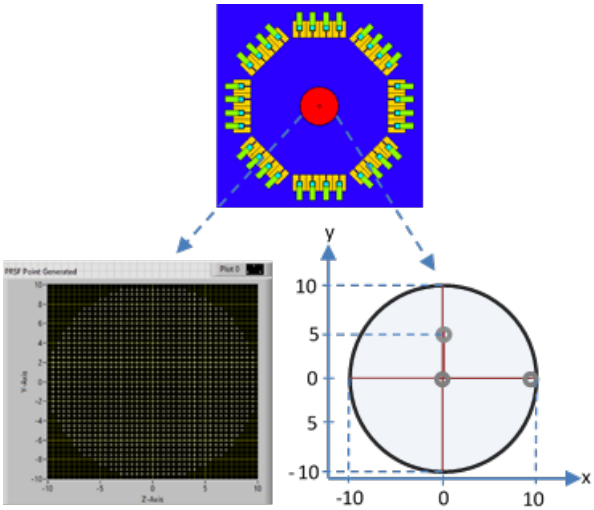

Figure 3: (a) 1245-point-source response generated inside ROI and (b) Different static point-source placement for positional accuracy detection.

For all three iSPECT arrangement, detection of positional accuracy of at static Cesium Cs-137, point-source is made by reconstructing the image for the source at the centre of ROI, 5 cm along the radius and 10 cm, which is at the edge of the ROI (grey circle in Figure 3b). Next, to determine the system's ability to differentiate two separated point-source, two equal strength sources are placed at 5 cm left and right of the origin. All of the image reconstruction processes were carried out using ML-EM software developed via LabVIEW. The calculation time for all of the reconstructed image was below 1s for each image.

3. RESULT AND DISCUSSION

3.1 Point-source Simulation

Figure 4 shows nine reconstructed images results from three different arrangements of the iSPECT system and three different placements of static point-source. The three rows of horizontal images represent the different arrangement of the iSPECT system with (a) hexagonal, (b) octagonal and (c) nonagonal structure. Meanwhile, the three vertical images represent different placement of point-source where (i) point-source at the origin, (ii) point-source at 5 cm from the origin and finally (iii) point-source at 10 cm from the origin, also represent source at the edge of the ROI. The green circle is the reference for the circumference of the ROI with a radius of 10 cm. The brighter pixel represents the higher probability of finding the origin of the gamma radiation or source, and the darker represents the absence of gamma radiation.

The images in Figure 4 shows all of the three systems simulated can accurately detect point-source at the three different positions stated. The bright white pixel in the reconstructed images defines the detection of the point-source position reconstructed from the simulation. The sharper white pixel means more precise the detection of the point-source. Meanwhile, darker/blue images surrounding the point-source is represent as the noise for these reconstructed images. The fewer blue images mean better quality of the reconstructed images. From all three arrangements, the hexagonal arrangement of the iSPECT system has better reconstructed images for all three positions with less noise in the reconstructed images for the point-source detection. This result shows that the more numbers of the detector in an array, the better for the iSPECT system in imaging the point-source position. The result also shows that for all three arrangements, reconstructed images for point-source at the edge of the ROI has the sharpest white dot with less noise. The better detection of point-source position near the edge is due to near the edge of ROI; the position of the point-source is biased to a particular detector which makes it easier to locate the position and less noise in the reconstruction of the image.

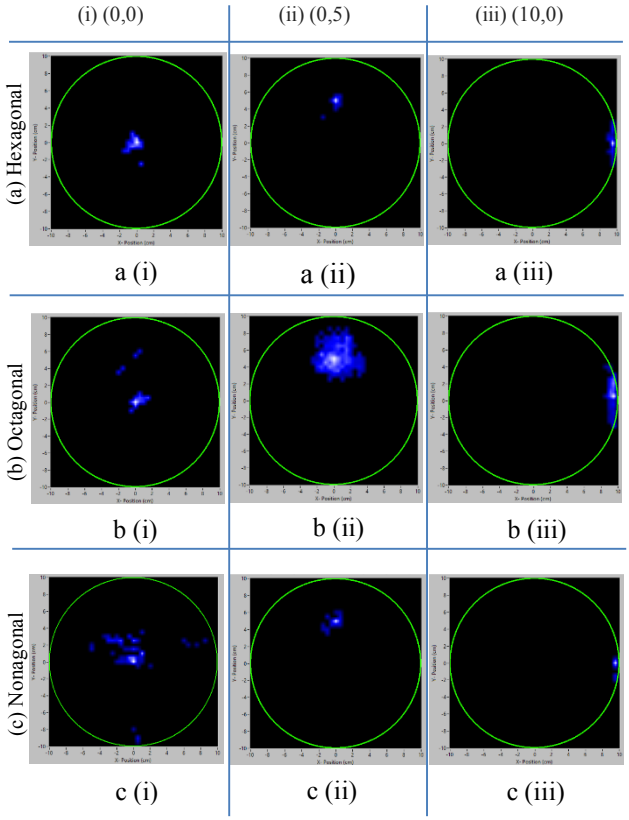

Figure 4: Reconstructed images for (a) Hexagonal, (b) Octagonal and (c) Nonagonal with (i) point-source at origin (0,0), (ii) point-source at 5 cm from origin (0,5) and (iii) point-source at 10 cm from origin (10,0).

Figure 5 is the profile plot of point-source at the origin for the three iSPECT systems at the position, y=0. The graph shows all three systems have the intensity peak at x=0, which confirm the position of the origin of the point source. The FHWM of the profile plot is calculated at half of the peak intensity, which is considered as the image resolution for the reconstructed image of each system [4]. The FWHM for the hexagonal, octagonal and nonagonal system is 1.25, 1.1 and 0.95, respectively. Although the reconstructed images for nonagonal have more noise, the FHWM of the profile plot at y=0 proves that the nonagon

system has better image resolution for point source imaging.

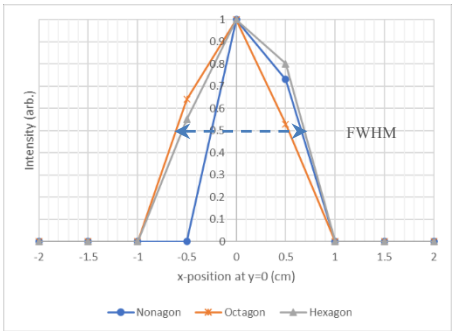

Figure 5: Profile plot of pixel intensity at y=0 for point-source at origin (0,0)

3.2 Two Point-source Simulation

Figure 6 shows reconstructed images for two point-source images of equal strength for all three iSPECT arrangement with (a) hexagonal, (b) octagonal and (c) nonagonal system. The dotted red circle is the positional reference of the actual position of the two point-source placed in the simulation. The results show only the nonagon system (Figure 5c) are able to detect the position of two point-source at their correct position with equal intensity. For the hexagon system, the reconstructed images only located one of the point-source in the vicinity of the actual position. In contrast, the octagonal system can only map the two point-source as distributed along the x-axis. The result also shows that, although only the nonagon iSPECT system can detect the two point-source in the simulation, all three reconstructed images have shown the intensity mapping has two clusters of intensity along the x-axis, which is the correct axis for the two point-source placements.

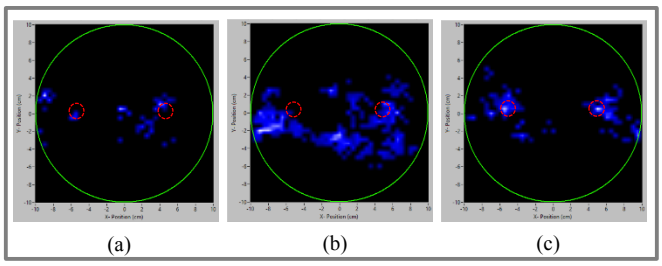

Figure 6: Reconstructed images for two point-source at (-5,0) and (0, 5) for (a) hexagonal, (b) octagonal and (c) nonagonal arrangement of iSPECT system.

4. CONCLUSION

In the present study, three different arrangement of iSPECT system has been modelled and simulated its ability to map a static single and two point-source images. The result shows that all three arrangements are able to detect the single point source at the origin (0,0), 5 cm from the origin (5,10) and near the edge of ROI at (0,10). From the three systems, the reconstructed images of the hexagonal arrangement have less noise. At the same time, regardless of the noise, the nonagon arrangement has a better overall image resolution than the other two systems. For the two point-source detections, the reconstructed images clearly show only the nonagon arrangement of the iSPECT system can detect the two sources' position. From this result, it can be concluded that the nonagon arrangement of the iSPECT system is the best for imaging the 20 cm ROI for point-source detection. Further study on the detection process will be done for different radiotracer sources and source shape to improve the iSPECT system for application in the industrial environment.

ACKNOWLEDGMENT

The authors would also like to extend the appreciation to all personnel of the Plant Assessment Technology (PAT) group, Industrial Technology Division, Malaysian Nuclear Agency.

REFERENCES

[1] S. Legoupil, G. Pascal, D. Chambellan, D. Bloyet, "An experimental single-photon emission computed tomograph method for dynamic 2D Fluid Flow analysis". *Appl. Radiat. Isot*. 48, 1507–1514, 1997.

[2] C. H. Mesquita, A. F. Velo, W. P. Calvo, D. V. Carvalho, M. M. Hamada, "Emission and transmission tomography system applied to analyze industrial process inside chemical reactors", *Nuclear Inst. And Methods in Physics Research, A*. vol. 954, p. 161847, 2020.

[3] J. G. Park, S. H. Jung, J. B. Kim, J. Moon, Y. S. Yeom, C. H. Kim, "Performance evaluation of advanced industrial SPECT system with diverging collimator". *Applied Radiation and Isotopes* 94, 125–130, 2014.

[4] J. G. Park, C. H. Kim, M. C. Han, S. H. Jung, J. B. Kim, and J. Moon. "Optimization of detection geometry for industrial SPECT by Monte Carlo simulations." *Journal of Instrumentation* 8, no. 04 2013.

[5] J. G. Park, S.H. Jung, J.B. Kim, J. Moon, M. C. Han, C. H. Kim, "Development of advanced industrial SPECT system with 12-gonal diverging-collimator". *Applied Radiation and Isotopes*. 89, 159–166, 2014.

[6] D. B. Pelowitz, J. W. Durkee, J. S. Elson, M. L. Fensin, J. S. Hendricks, M. R. James, R. C. Johns et al. MCNPX User's Manual 2.6 extensions. No. LA-CP-07-1473. Los Alamos National Lab. (LANL), Los Alamos, NM (United States), 2008.

[7] International Atomic Energy Agency, "Industrial Process Gamma Tomography". IAEA TECDOC-1589. International Atomic Energy Agency, 2008.

[8] P. P. Bruyant, "Analytic and iterative reconstruction algorithms in SPECT". *J Nucl Med.* 43(10), 1343-1358, 2002.

[9] M. N. Wernick, and J. N. Aarsvold. Emission tomography: the fundamentals of PET and SPECT. *Elsevier*, 2004.